DETERMINATION OF VERTICAL AND HORIZONTAL PERMEABILITIES FOR VERTICAL OIL AND GAS WELLS WITH PARTIAL COMPLETION AND PARTIAL PENETRATION USING PRESSURE AND PRESSURE DERIVATIVE PLOTS WITHOUT TYPE-CURVE MATCHING

Katherine Moncada[1], Djebbar Tiab[2], Freddy-Humberto Escobar*[3], Matilde Montealegre[3], Abel Chacon[4], Renzon Zamora[3] and Sandra-L. Nese[3]

[1]Schlumberger
[2]University of Oklahoma
[3]Universidad Surcolombiana , Programa de Ingeniería de Petróleos, Grupo de Investigación en Pruebas de Pozos
[4]WoodGroup
e-mail: fescobar@usco.edu.co

I t has been long recognized that in some reservoirs the flow does not follow the expected radial cylindrical pattern. Spherical flow may take place in systems with wells completed in thick reservoirs where a short completion interval is open to flow yielding a unique and more complex early-time pressure behavior. Some of the main reasons for partial penetration are to avoid coning of water and minimize sand production. A similar early-time pressure behavior may be due to the presence of plugged perforations. Such well completions are referred to as limited-entry, restricted-entry or partially penetrating wells. A typical case of spherical propagation of pressure transients occurs during the repeat formation tester measurements. Such a test measures spot formation pressures and recovers formation fluid samples for gaining an insight into the reservoir flow mechanics.

The purpose of this study is to identify on the pressure and pressure derivative curves the unique characteristics for different flow regimes resulting from these type of completions and to determine various reservoir parameters, such as vertical, horizontal permeability, and various skin factors. The interpretation is performed using Tiab's Direct Synthesis (*TDS*) Technique, introduced by Tiab (1993), which uses analytical equations obtained from characteristic lines and points found on the log-log plot of pressure and pressure derivative to determine permeability, skin and wellbore storage without using type-curve matching. The extension of this methodology for the case under study includes wellbore storage and skin effects. It is applied to both drawdown and buildup tests.

We found that a spherical or hemispherical flow regime occurs prior to the radial flow regime whenever the penetration ratio of about 20%. A half-slope line on the pressure derivative is the unique characteristic identifying the presence of the spherical/hemispherical flow. The typical half-slope line of theses flow regimes is used to estimate spherical permeability and spherical skin values. These parameters are then used to estimate vertical permeability, anisotropy index and skin. Results of *TDS* technique where successufully compared to those of conventional technique for field and simulated examples.

Keywords: *hemispherical flow, spherical flow, radial flow, skin factor, analytical solution, difussivity equation.*

* To whom correspondence may be addressed

Desde hace mucho tiempo se sabe que en algunos yacimeintos el flujo no sigue la trayectoria cilíndrica esperada. El flujo esférico puede ocurrir en sistemas con pozos completados en formaciones con mucho espesor con una pequeña porción de intervalo perforado abierto al flujo dando lugar a una única y más compleja respuesta de presión temprana. Algunas de las principales razones para acudir a penetración parcial es evitar la conificación de agua y minimizar la producción de arena. Un comportamiento similar de la presión a tiempos tempranos podría deberse al taponamiento en las perforaciones. Tales completamientos se denominan entrada limitada, entrada restringida o pozos con penetración parcial. Un caso típico de propagación esférica del transiente de presión ocurre durante medidas de RFT. Dicho registro mide presiones de formación y muestrea los fluidos de la formación para tener una idea de la mecánica de flujo en el yacimiento.

El propósito de este estudio es identificar características únicas en le gráfico de la presión y la derivada para diversos regimenes de flujo que resultan de este tipo de completamientos y determinar los distintos parámetros del yacimiento. Tales como permeabilidad vertical, permeabilidad horizontal, y diversos factores de daño. La interpretación se lleva a cabo usando la *Tiab's Direct Synthesis (TDS) Technique*, introducida por Tiab (1993), la cual usa ecuaciones analíticas obtenidas de líneas y puntos característicos hallados en el gráfico log-log de presión y derivada de presión para determinar permeabilidad, daño y almacenamiento sin emplear curvas tipo. La extensión de esta metodología para el caso en estudio incluye almacenamiento y daño. La técnica se aplica tanto a pruebas de restauración como de declinación de presión.

Encontramos que el flujo hemisférico o esférico toma lugar antes del flujo radial siempre que la relación de penetración sea aproximadamente menor del 20%. Una pendiente negativa de ½ en la curva de la derivada es la característica única para identificar la presencia de flujo hemisférico/esférico. Esta línea típica de pendiente $-\frac{1}{2}$ se usa para determinar la permeabilidad esférica y los daños esféricos, para luego estimar la permeabilidad vertical y el índice de anisotropía. Los resultados de la *TDS* fueron satisfactoriamente comparados con casos de campo y casos simulados.

Palabras claves: *flujo hemisférico, flujo esférico, flujo radial, factor de daño, solución analítica, ecuación de difusividad.*

NOMENCLATURE

b	Fractional penetration ratio, h_p/h, dimensionless
B	Formation volume factor, res vol/stb vol
C	Wellbore storage coefficient
C_D	Dimensionless wellbore storage coefficient
c_f	Rock compressibility, psi-1
c_o	Oil compressibility, psi-1
c_t	Total reservoir compressibility, psi-1
G	Function of the fractional penetration ratio
h	Total formation thickness, ft
h_p	Limited interval open to flow, ft
h_D	Dimensionless total formation thickness
I_A	Anisotropy index, dimensionless
k	Reservoir permeability, md
k_H	Horizontal permeability, md
k_V	Vertical permeability, md
k_{sp}	Spherical permeability, md
k_{hs}	Hemispherical permeability, md
k_{r1}	Horizontal permeability from first radial flow, md
k_{r2}	Horizontal permeability from second radial flow, md
$m(P)$	Pseudopressure, psi^2/cp
P	Pressure, psia
P_D	Dimensionless pressure
P_i	Initial reservoir pressure, psia
P_{wf}	Well flowing pressure, psia
q	Oil rate, STB/D
q_g	Gas rate, Mscf/D
r	Radial distance, ft
r_D	Dimensionless radial distance
r_w	Wellbore radius, ft
r_{sw}	Spherical wellbore radius, ft
s_m	Mechanical or damage skin
s_m	Mechanical or damage pseudoskin (gas wells)
s_c	Partial penetration-skin
s_t	Total skin
t	Testing time, h
T	Reservoir temperature, °R
t_D	Dimensionless time

NOMENCLATURE

z	Gas deviation factor
$\varnothing$	Porosity, fraction
μ	Oil viscosity, cp

SUBSCRIPTS

D	Dimentionless quantity
g	Gas
H	Horizontal
i	Initial
N	Unit slope
r	Radial flow
$r1$	First or early radial flow
$r2$	Second or late radial flow
s_p	Spherical flow
h_s	Hemispherical flow
V	Vertical

SI METRIC CONVERSION FACTOR

Bbl x 1.589 873	E-01 = m3
cp x 1.0*	E-03 = Pa-s
ft x 3.048*	E-01 = m
ft2 x 9.290 304*	E-02 = m2
psi x 6.894 757	E+00 = kPa
λ	Interporosity flow parameter

INTRODUCTION

The most common practice to analyze pressure transient data is to assume a radial flow profile. However, in wells with partial penetration/completion a hemispherical/spherical flow is more representative of the system.

In reality the formation itself is usually nonuniform or heterogeneous in properties such as porosity and permeability, both areally and vertically resulting from deposition, folding or faulting. The vertical anisotropy is fundamental in describing pressure response around a well partially penetrating a formation unbounded laterally and confined at the top and bottom by impermeable layers.

In this work the effect of partial well completion and partial well penetration on pressure behavior will be analyzed in order to determine vertical permeability, horizontal permeability, skin and wellbore storage. The

knowledge of vertical anisotropy would allow a better reservoir development and subsequent secondary recovery programs could be planned more efficiently.

Spherical symmetries are appropriate in well pressure analyses when the well does not fully penetrate the productive horizon, or perhaps if it were selectively completed. Muskat presented the problem of steady state spherical flow in 1932.

Several papers, although not enough, have been written to discuss spherical flow phenomena but mostly in connection with wireline formation testing tools. Moran and Finklea in 1962 were the first to suggest that a pressure buildup equation based on spherical flow was necessary to correctly analyze pressure data obtained from a wireline formation tester (a limited entry test). The first general discussion of unsteady-state spherical flow appears to be a paper published by Chatas in 1966. In 1974, Culham presented equations suitable for pressure buildup analysis but the wellbore storage distortion was not included.

Raghavan and Clark (1975) examined the applicability of the spherical flow equations given by Moran and Finklea (1962) to a well producing from a limited section of a thick anisotropic formation. Later in 1980, Brigham *et al*. extended the Chatas (1966) study to include wellbore storage effects. However, their solution is valid only for the case of no wellbore damage. Later, Joseph (1984) and Proett (1998) presented solutions including wellbore storage and damage skin effects. Additional references discussing the partial penetration problem are available from the literature (Brons and Marting, 1961; Abbot *et al.*, 1978). However, their main concern was to express the partial penetration and limited entry as a skin factor not to estimate vertical permeability.

In 1993, Tiab introduced the *TDS* Technique for interpreting log-log pressure and pressure derivative plots by using analytical solutions to determine permeability, skin and wellbore storage without employing type-curve matching. This revolutionary technique, already extended to many other systems (Boussalem, *et al.*, 2002; Tiab and Escobar, 2003), uses such unique features as lines, intersection points, and other "fingerprint" characteristics found on the pressure and pressure derivative log-log plot to develop analytical equations to readily obtain reservoir parameters. The main objective of this paper is to extend *TDS* Technique for the case of wells with partial penetration and partial completion.

FLOW GEOMETRIES

Vertical wells can exhibit different flow regimes during their transient behavior. Spherical flow can occur when a well is producing from a limited section of a thick reservoir or producing from a thick reservoir under a variety of conditions such as the presence of shale barriers spherical flow will also develop. In the case of partial completion in thick reservoirs.

Spherical flow can be visualized as flow along the radius of a sphere. Figure 1 shows the ideal geometry of spherical flow and demonstrates the concept of perfect radial flow towards a common point in the sphere: its center. Hemispherical flow, also shown in Figure 1, is identical to spherical flow with the obvious exception that the flow is contained within a hemisphere.
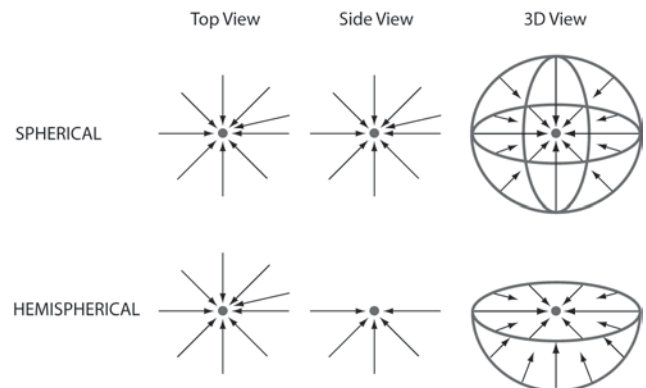

Figure 1. Ideal geometry of spherical and hemispherical flow

In practice, the flow is not purely spherical or hemispherical because the completion interval is not a true point sink. However, the flow is spherical in a practical sense if the completion interval is very short relative to the net pay. In the case of a thick reservoir between two impermeable confining layers and a short partial-completion interval, the spherical flow regime will occur between two periods of cylindrical-radial flow. In both cases, three flow periods can be identified -additional to wellbore storage- as follows: A period 1 corresponding to an initial radial flow over the completion interval. Dur-

ing this period the reservoir behaves as if the formation thickness were equal to the length of the open zone. A Period 2 corresponds to a transition period during which spherical/hemispherical flow may be identified. And the third period corresponds to a second radial flow but this time over the total formation thickness.

MATHEMATICAL FORMULATION

The fundamental partial differential equation (Muskat, 1932) describing the flow of a slightly compressible fluid in a homogeneous and infinite porous medium characterized by a spherical geometry, can be stated as:

$$\frac{1}{r^2}\frac{\partial}{\partial r}\left(r^2\frac{\partial \Phi}{\partial r}\right)+\frac{1}{r^2\sin\theta}\frac{\partial}{\partial \Phi}\left(\sin\theta\frac{\partial \Phi}{\partial \theta}\right)+\frac{1}{r^2\sin^2\theta}\frac{\partial^2\Phi}{\partial \chi^2}=\frac{\phi\,\mu c_t}{k}\frac{\partial P}{\partial t}$$

(1)

Several authors (Moran and Finlklea, 1962) have presented solutions to *Equation 1* for different flowing conditions, fluid types and boundary conditions. For the purpose of this study, besides the basic considerations normally assumed in well test analysis, Joseph (1984) also assumed the three following considerations:

1) The flow is perfectly spherical to a well of radius r_w in an isotropic medium, then the terms $\partial\Phi/\partial\theta$ and $\partial\Phi/\partial\chi$ can in *Equation 1* can be dropped. Therefore, *Equation* 1 can be stated as:

$$\frac{1}{r^2}\frac{\partial}{\partial r}\left(r^2\frac{\partial P}{\partial r}\right)=\frac{\phi\,\mu c_t}{k}\frac{\partial P}{\partial t}$$

(2)

2) Even though Joseph (1984) assumed the medium is spherically isotropic; hence k in *Equation 2* is the constant spherical permeability. The analysis in systems possessing simple anisotropy (i.e., uniform but unequal horizontal and vertical permeability components) can be also done without significatively affecting the radial coordinate (Joseph, 1984). In that case, k should be replaced by k_{sp} in *Equation 2*.

$$\frac{1}{r^2}\frac{\partial}{\partial r}\left(r^2\frac{\partial P}{\partial r}\right)=\frac{\phi\,\mu c_t}{k_{sp}}\frac{\partial P}{\partial t}$$

(3)

where k_{sp} is set as a geometric average of the permeability components as follows:

$$k_{sp}=\sqrt[3]{k_{xx}k_{yy}k_{zz}}$$

(4)

and assuming an areally isotropic system then:

$$k_{sp}=\sqrt[3]{k_V k_H^2}$$

(5)

3) The physical system of interest considers a sphere itself instead of its center. This region of singularity is called a continuous "spherical sink" which corresponds physically to a wellbore, which must be visualized as a sphere. Hence, the cylindrical wellbore of radius r_w must be represented by a fictitious spherical wellbore of radius r_{sw} given by an equation originally suggested by Moran and Finklea (1962):

$$r_{sw}=\frac{h_p}{2\ln\left(h_p/r_w\right)}$$

(6)

h_p has to be greater or equal than r_w. Under the above assumptions the spherical source solution for long time is given then by:

$$P_{Dsp}\left(t_{Dsp}\right)=1-\frac{1}{\sqrt{\pi\,t_{Dsp}}}+s$$

(7)

Where the dimensionless variables suggested by Joseph (1984) for spherical flow are defined in a field units as follows:

$$P_{Dsp}=\frac{4\pi k_{sp}r_{sw}}{q\mu}\left(P_i-P_{r,t}\right)$$

(8.a)

$$t_{Dsp}=\frac{k_{sp}r_{sw}^2 t}{\phi\,\mu c_t r^4}; r\geq r_{sw}$$

(9.a)

$$r_{Dsp}=1-\frac{r_{sw}}{r}; r\geq r_{sw}$$

(10.a)

$$C_{Dsp}=\frac{C}{4\pi\phi c_t r_{sw}^3}$$

(11.a)

and the dimensionless variables normally used in radial coordinates are (Earlougher, 1977):

$$P_{Dr}=\frac{k_r h}{2\pi q\mu B}\Delta p$$

(8.b)

$$t_{Dr}=\frac{k_r t}{\phi\,\mu c_t r_w^2}$$

(9.b)

$$r_D=1-\frac{r_{sw}}{r}; r\geq r_{sw}$$

(10.b)

$$C_D=\frac{C}{2\pi\,\phi\,c_t h r_w^2}$$

(11.b)

Characteristic points and lines

A log-log plot of dimensionless pressure and pressure derivative versus time is shown in Figure 2. Although, wellbore storage may be present, the three dominant flow regimes identified in a well with partial completion in chronological order are: early radial, spherical and late radial flows (Moncada, 2004).
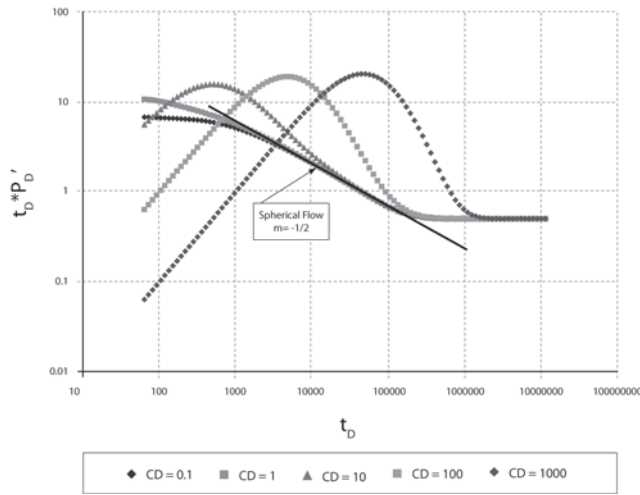

Figure 2. Pressure derivative with wellbore storage and no mechanical skin

(1a) Wellbore storage. The first characteristic observed in Figure 3 corresponds to pure wellbore storage flow. The dimensionless wellbore pressure approximation for short time governed by spherical geometry (Joseph, 1984) is given by:

$$P_D(t_D) = \frac{t_D}{C_D}; s \geq 0; C_D > 0 \qquad (12)$$

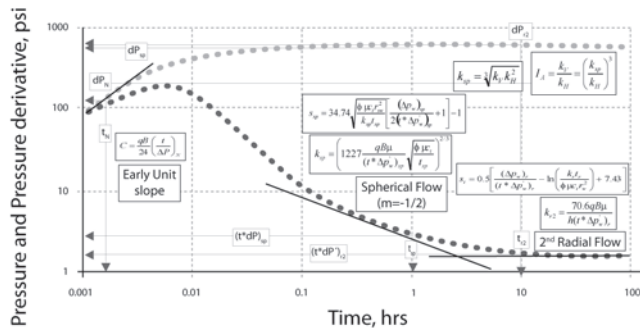*Equation 12* is the well known formulation for wellbore depletion which is identical to the results

obtained for cylindrical and linear flow. This results in the familiar unit-slope portion on the log-log plot at early times. Combination of *Equations 9.a* and *11.a* will lead to:

$$\frac{t_D}{C_D} = \left(\frac{5.90 * 10^{-4} r_{sw} k_{sp}}{\mu} \right) \frac{t}{C} \qquad (13)$$

Substituting *Equation 13* and *Equation 8.a* into *Equation 12* and solving explicitly for *C* we obtained:

$$C = \frac{qB}{24} \left(\frac{t}{\Delta P} \right)_N \qquad (14)$$

Where t_N is any convenient time during the unit-slope portion on the log-log plot and ΔP is the value of pressure drop corresponding to t_N.

(1b) Early radial flow. This flow period is usually short and masked by the wellbore storage, but if a downhole shut-in tool is used, then the analysis of this flow regime utilizes the normal radial flow equations. Taking into account that during this period the pressure response behaves as if the formation thickness is equal to the length of the open zone, h_p. According to this the following equations will apply (Tiab, 2003):

$$k_{r1} = \frac{70.6qB\mu}{h_p(t*\Delta P')_{r1}} \qquad (15)$$

$$s_{r1} = 0.5 \left[\frac{(\Delta P_w)_{r1}}{(t*\Delta P')_{r1}} - \ln \left(\frac{k_r t_{r1}}{\phi \mu c_t r_w^2} \right) + 7.43 \right] \qquad (16)$$

The subscript $r1$ stands for first radial flow line. Where t_{r1} is any convenient time during the first radial flow regime on the log-log plot. ΔP_{r1} and $(t*\Delta P')_{r1}$ are the values corresponding to t_{r1}.

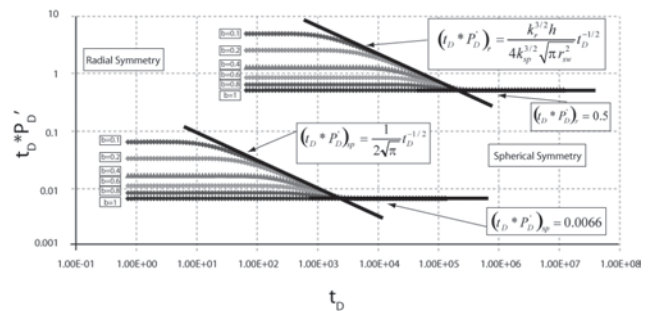Figure 3. Pressure response in a well with partial completion

Figure 4. Pressure derivative type curves for a vertical well with partial completion for different penetration ratios ($b = h_p/h$) in radial and spherical symmetry

(1c) Intersection point. As shown in Figure 4, for analytical simulation runs using their respective co-ordinate systems, the -½-slope line corresponding to the spherical flow and the late radial flow line of the dimensionless pressure derivative in spherical symmetry intersect at:

$$\left(t_D * P_D '\right)_i = \frac{1}{2\sqrt{\pi t_{Dsp}}}$$

$$\left(t_D * P_D '\right)_i = 0.0066$$

Equating the above two expression will yield:

$$\frac{1}{2\sqrt{\pi}} t_{Dsp}^{-1/2} = 0.0066$$

Substituting *Equation 9.a* into the above expression and solving for the intersection time in field units, it yields:

$$t_i = 6927748.85 \frac{\phi \mu c_t r_{sw}^2}{k_{sp}} \tag{17.a}$$

Equation 17.a can be used to estimate either r_{sw} or k_{sp}. Another equation to define this intersection time can be found from the -½-slope line corresponding to the spherical flow and the late radial flow line of the dimensionless pressure derivative, but this time in radial symmetry. Knowing from Figure 4 that:

$$\left(t_D * P_D '\right)_i = \frac{k_r^{3/2} h}{4 k_{sp}^{3/2} \sqrt{\pi r_{sw}^2}} \frac{1}{\sqrt{t_{Dr}}}$$

$$\left(t_D * P_D '\right)_i = 0.5$$

At the intercept the above equations are equal, then:

$$\frac{k_r^{3/2} h}{4 k_{sp}^{3/2} \sqrt{\pi r_{sw}^2}} \frac{1}{\sqrt{t_{Dr}}} = 0.5 \tag{17.b}$$

In radial geometry, the dimensioness pressure derivative and time, respectively, defined in field units are:

$$\left(t_D * P_D '\right)_r = \frac{k_r h}{141.2 q \mu B} \left(t * \Delta P'\right) \tag{18}$$

$$t_{Dr} = \frac{0.0002637 kt}{\phi \mu c_t r_w^2} \tag{19}$$

Now, substituting *Equation 19* into *Equation 17.b* and solving for the intersection time, t_i, in field units:

$$t_i = 301.77 \frac{k_r^2 h^2 \phi \mu c_t}{k_{sp}^3} \tag{20}$$

Combining *Equations 17.a* and *20* leads to:

$$r_{sw} = 0.0066 \frac{k_r h}{k_{sp}} \tag{21}$$

(2a) Spherical flow. From the dimensionless wellbore pressure approximation governed by spherical geometry (Joseph, 1984), *Equation 7*, the dimensionless pressure derivative is given by:

$$P_D ' = \frac{1}{2\sqrt{\pi}} \frac{1}{t_D^{3/2}} \tag{22}$$

$$\left(t_D * P_D '\right) = \frac{1}{2\sqrt{p}} t_D^{-1/2} \tag{22.a}$$

Taking logarithm to both sides of the above expression:

$$\log \left(t_D * P_D '\right) = -\frac{1}{2}\log t_D + \log \frac{1}{2\sqrt{\pi}} \tag{23}$$

The slope of this straight line is -½, which is a unique characteristic of spherical flow regime. Substituting the dimensionless terms in *Equation 23* and solving for the pressure derivative it results:

$$\left(t * \Delta P'\right) = \frac{1}{2} m_{sp} t^{-1/2} \tag{24}$$

being,

$$m_{sp} = 2453 \frac{q \mu B}{k_{sp}} \left(\frac{\phi \mu c_t}{k_{sp}}\right)^{1/2} \tag{25}$$

Taking logarithm to both sides of *Equation 24* gives:

$$\log \left(t * \Delta P'\right) = -\frac{1}{2}\log t + \log \left(\frac{1}{2} m_{sp}\right) \tag{22.b}$$

This expression shows that a plot of measured *t*ΔP'* versus time on a log-log graph will yield a straight line of slope −½ when spherical flow is dominant. Combining *Equations 24* with *25* and solving for k_{sp} yields:

$$k_{sp} = \left(1227 \frac{q B \mu}{(t * \Delta P')_{sp}} \sqrt{\frac{\phi \mu c_t}{t_{sp}}}\right)^{2/3} \tag{26}$$

Substituting the dimensionless groups in *Equation 7* will yield:

$$\Delta P = m_{sp1} - m_{sp}t^{-1/2} + m_{sp1}s_{sp} \qquad (27)$$

where;

$$m_{sp1} = \frac{70.6q\mu B}{k_{sp}r_{sw}}$$

$$m_{sp} = 2453\frac{q\mu B}{k_{sp}}\left(\frac{\phi\,\mu c_t}{k_{sp}}\right)^{1/2}$$

An expression relating the spherical flow portion of the pressure and the pressure derivative can be derived by dividing *Equation 24* with *Equation 27* to yield:

$$\frac{\Delta P}{(t*\Delta P')} = 2\left[\frac{m_{sp1}}{m_{sp}t^{-1/2}} + \frac{m_{sp1}s_{sp}}{m_{sp}t^{-1/2}} - 1\right] \qquad (28)$$

Solving for the spherical skin, s_{sp}, the following *Equation* is obtained:

$$s_{sp} = 34.74\sqrt{\frac{\phi\,\mu c_t r_{sw}^2}{k_{sp}t_{sp}}}\left[\frac{(\Delta P)_{sp}}{2(t*\Delta P')_{sp}} + 1\right] - 1 \qquad (29)$$

The subscript *sp* stands for spherical flow. ΔP_{sp} and $(t*\Delta P')_{sp}$ are the values of pressure and pressure derivative corresponding to an arbitrary value of t_{sp} on the spherical flow straight line.

(2b) Hemispherical flow. This is considered as a special case of spherical flow, and it should be realized that all results developed under spherical flow extend over directly for hemispherical flow applications with only minor modifications. The obvious observation is that the flow is now contained within a hemisphere

Figure 5. Pressure Response in a well with partial penetration illustrating characteristic points and lines

instead of a sphere. Then, *Equation 2* also applies to hemispherical flow and the dimensionless pressure derivative will be then equal to the one for spherical flow (*Equation 22*). It should also be noted that the suffix *sp* ought to be changed by *hs* indicating hemispherical flow. Figure 5 shows a log-log plot of the pressure and pressure derivative versus dimensionless time for a partial penetrated well. This is then to the one for spherical flow (*Equation 22*). The dimensionless variables suggested by Joseph (1984) will differ only by replacing the geometric factor 4π by 2π. *Equation 22.a* corresponds to the early-time straight line. The slope of this straight line is also -½. Again, substituting the dimensionless terms in *Equation 22.a* and solving for the pressure derivative, it yields:

$$(t*\Delta P') = \frac{1}{2}m_{hs}t^{-1/2} \qquad (30)$$

where:

$$m_{hs} = 4906\frac{q\mu B}{k_{hs}}\left(\frac{\phi\,\mu c_t}{k_{hs}}\right)^{1/2} \qquad (31)$$

Taking logarithm to both sides of *Equation 30* gives:

$$\log(t*\Delta P') = -\frac{1}{2}\log t + \log\left(\frac{1}{2}m_{hs}\right) \qquad (32)$$

Also, a plot of $t*\Delta P'$ versus t on a log-log graph will yield a straight line of slope −½ when hemispherical flow is dominant. Combining *Equations 30* and *31* and solving for k_{hs} yields:

$$k_{hs} = \left(2453\frac{qB\mu}{(t*\Delta P')_{hs}}\sqrt{\frac{\phi\,\mu c_t}{t_{sp}}}\right)^{2/3} \qquad (33)$$

where;

$$k_{hs} = \sqrt[3]{k_V k_H^2} \qquad (34)$$

Substituting the dimensionless terms in *Equation 7* leads to:

$$\Delta P = m_{hs1}(1+s) - m_{hs}t^{-1/2} \qquad (35)$$

being:
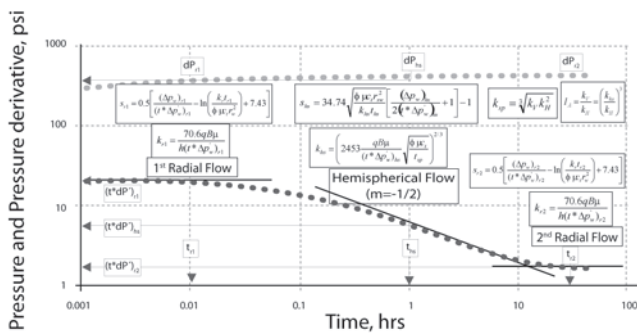
$$m_{hs1} = \frac{141.2q\mu B}{k_{hs}r_{sw}} \qquad (36)$$

$$m_{hs} = 4906 \frac{q\mu B}{k_{hs}} \left(\frac{\phi \mu c_t}{k_{hs}} \right)^{1/2}$$
(37)

An expression relating the hemispherical flow portion of the pressure and the pressure derivative can be obtained by dividing *Equation 35* with *Equation 30*, thus:

$$\frac{\Delta P}{(t*\Delta P')} = 2 \left[\frac{m_{hs}}{m_{hs} t^{-1/2}} + \frac{m_{hs1} s}{m_{hs} t^{-1/2}} - 1 \right]$$
(38)

Solving for the skin, s_{hs}, the following *Equation* is obtained:

$$s_{hs} = 34.74 \sqrt{\frac{\phi \mu c_t r_{sw}^2}{k_{hs} t_{hs}}} \left[\frac{(\Delta P)_{hs}}{2(t*\Delta P')_{hs}} + 1 \right] - 1$$
(39)

Where ΔP_{hs} and $(t*\Delta P')_{hs}$ are the values corresponding to any arbitrary time, t_{hs}, on the hemispherical flow straight line.

(2c) Intersection point. As shown in Figure 6, for analytical simulation runs using their respective coordinate systems, the negative half-slope line corresponding to the hemispherical flow and the late radial flow line of the dimensionless pressure derivative in hemispherical symmetry intersect at:

$$\left(t_D * P_D ' \right)_i = \frac{1}{2\sqrt{\pi t_{Dsh}}}$$

$$\left(t_D * P_D ' \right)_i = 0.0033$$

Equating the above two expression will yield:

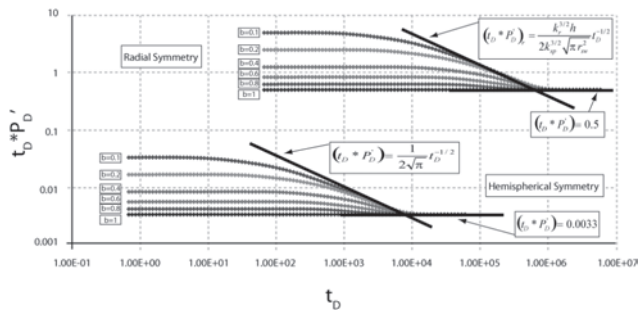$$\frac{1}{2\sqrt{\pi}} t_{Dsh}^{-1/2} = 0.0033$$

Figure 6. Pressure derivative type curves for a vertical well with partial penetration in radial and hemispherical symmetry

Substituting an expression similar to *Equation 9.a* in hemispherical coordinates into the above expression and solving for, t_i, the intersection time in field units, it yields:

$$t_i = 27710995.41 \frac{\phi \mu c_t r_{sw}^2}{k_{hs}}$$
(40.a)

Equation 40.a can be used to estimate either r_{sw} or k_{hs}. Another equation to define this intersection time can be found from the -½-slope line corresponding to the hemispherical flow and the late radial flow line of the dimensionless pressure derivative but, this time, in radial symmetry. From Figure 6 we know that:

$$\left(t_D * P_D ' \right)_i = \frac{k_r^{3/2} h}{2 k_{hs}^{3/2} \sqrt{\pi r_{sw}^2}} \frac{1}{\sqrt{t_{Dr}}}$$
(40.b)

$$\left(t_D * P_D ' \right)_i = 0.5$$

At the intercept the above *equations* are equal, then:

$$\frac{k_r^{3/2} h}{2 k_{hs}^{3/2} \sqrt{\pi r_{sw}^2}} \frac{1}{\sqrt{t_{Dr}}} = 0.5$$
(41)

Substituting *Equation 19* into *Equation 40.b* and solving for t_i in field units:

$$t_i = 1207.09 \frac{k_r^2 h^2 \phi \mu c_t}{k_{hs}^3}$$
(42)

Combining *Equations 40.a* and *42* will yield:

$$r_{sw} = 0.0033 \frac{k_r h}{k_{hs}}$$
(43)

(3) Late radial flow. For the analysis of this flow regime the normal radial flow equation applies considering the total formation thickness. Permeability and mechanical skin can be calculated according to Tiab (2003):

$$k_{r2} = \frac{70.6 q B \mu}{h(t*\Delta P')_{r2}}$$
(44)

$$s_{r2} = 0.5 \left[\frac{(\Delta P)_{r2}}{(t*\Delta P')_{r2}} - \ln\left(\frac{k_r t_{r2}}{\phi \mu c_t r_w^2} \right) + 7.43 \right]$$
(45)

Subscript *r2* stands for the second radial flow line. Being t_{r2} any convenient time during the radial flow line on the log-log plot. ΔP_{r2} and $(t*\Delta P')_{r2}$ are the values corresponding to tr2.

Important considerations

One of the purposes of this study was to determine the range of values for the dimensionless wellbore storage, C_D based upon *Equation 11.b*, that can mislead the interpretation of spherical/hemispherical flow regime. A better understanding can be reached plotting (t_D*P_D') vs. t_D/C_D as shown in Figure 2. Notice that for values of $C_D < 10$, the -½-slope behavior can be easily identified while for C_D around 100, the -½ slope is more difficult to observe. Definitely, for $C_D > 100$, the spherical/hemispherical flow regime is completely masked by wellbore storage effects and this will make impossible to apply the method here established to calculate vertical permeability.
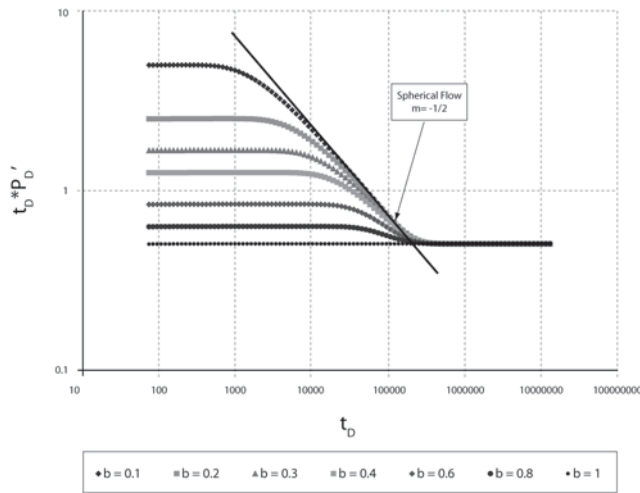

Figure 7. Pressure Derivative considering different lengths of partial penetration ($C_D = 0$, $s = 0$)

The length of the completed interval or the partial penetration length, h_p, also plays an important role on the definition of the spherical/hemispherical flow as described in Figure 7. The characteristic slope of -½ is absent for penetration ratios greater than 40 %.

TDS TECHNIQUE PROCEDURE

The following procedure can be used to calculate and verify values of C, k_{sp} or k_{hs}, k_H, k_V and st from a log-log plot of pressure and pressure derivatives versus time without type curve matching (Moncada, 2004).

Step 1. Plot pressure and pressure derivative on a log-log paper. If given the case, draw the early unit-slope line

corresponding to the *wellbore storage flow regime* and take any convenient t and ΔP values on the unit-slope line and estimate C from (Tiab and Escobar, 2003):

$$C = \frac{qB}{24}\left(\frac{t}{\Delta P}\right)_N \qquad (46)$$

If no wellbore storage effect is seen, an *initial radial flow regime* may develop. Then, the normal radial flow equations will apply, taking into account that during this period the pressure response behaves as if the formation thickness is equal to the length of the open interval, h_p. Permeability and skin can be calculated using *Equations 15* and *16*, respectively.

Step 2. Draw a straight line with slope of -½, characteristic of the *spherical/hemispherical flow regime*. Select any convenient time t_{sp} during spherical/hemispherical flow and read the corresponding value of $(t*\Delta P')_{sp}$. Then, k_{sp} (or k_{hs}) can be readily calculated using either *Equation 26* or *33*.

Step 3. Also from the -½-slope straight line the spherical or hemispherical skin, s_{sp} or s_{hs}, can be obtained using either *Equation 29* or *39*, respectively.

Step 4. From the infinite-acting line, select any convenient time t_r and read ΔP_r and $(t*\Delta P')_r$. Then, the value of radial permeability (horizontal permeability) and total skin factor can be calculated with *Equations 44* and *45*.

Step 5. k_V can be estimated using either *Equation 5* or *34*, for spherical or hemispherical flow regime, respectively.

Step 6. Calculate the anisotropy index, I_A, using *Equation 47*.

$$I_A = \frac{k_V}{k_H} = \left(\frac{k_{sp}}{k_H}\right)^3 \qquad (47)$$

Step 7. Knowing the mechanical and the total skin the partial penetration expressed as a skin factor can be calculated from:

$$s_t = \frac{s_m}{b} + s_c \qquad (48)$$

Step 8. For verification purposes, it is recommended to use either *Equations 17.a*, *20* and *21* (spherical flow) or *Equations 40.a*, *42* and *43* (hemispherical flow).

Note: This step-by-step procedure can also be applied to gas wells (Zamora and Nese, 2005) by changing *Equations 46, 15, 16, 26, 33, 29, 33, 44* and *45* (appearing chronologically in the procedure) by *Equations A.9* through *A.17*.

EXAMPLES

Field example 1

Table 1 contains drawdown test data taken from Abbott *et al.* (1978). Well No. 20 is partially completed in a massive carbonate reservoir. The well was shut-in for stabilization and then was flowing at 5200 BOPD for 8,5 h. Reservoir and fluid parameters are given in Table 1b.

Table 1b. Reservoir, well and rock data for field example 1

Property	Value	Property	Value
h, ft	302	r_w, ft	0,246
hp, ft	20	q, bpd	5200
ø, %	0,2	μ, cp	0,21
c_t, psi-1	34,2x10-6	Bo, rb/STB	1,7
Pi, psia	2298		

Solution

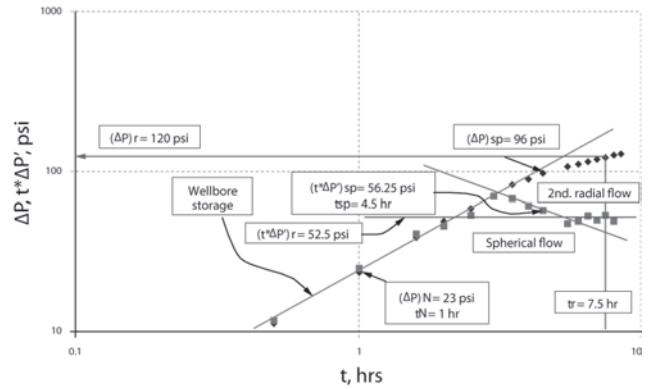Step 1. The pressure and pressure derivative plot is given in Figure 6. From the unit-slope line we read

Figure 8. Pressure and pressure derivative plot for Well No. 20, field example 1

$(\Delta P)_N$ =23 psi and t_N= 1 h. Then, *C* of 16,01 bbl/psi is calculated using *Equation 46*.

Step 2. $(t^* \Delta P')_{sp}$=56,25 psi, $(\Delta P)_{sp}$=96 psi and t_{sp} = 4,5 are read from the -½-slope line. ksp=8,05 md is found with E*quation 26*.

Step 3. Also from the -½-slope straight line a spherical mechanical skin, s_{sp} = -0,87 is obtained using *Equation 29*.

Step 4. From the *late radial flow regime*, t_{r2} = 7,5 h, ΔP_{r2} = 120 psi and $(t^* \Delta P')_{r2}$ = 52,2 psi are read, a value of the horizontal permeability of 8,26 md is estimated by means of *Equation 44* and a total skin factor of -5,33 is found with *Equation 45*.

Step 5. k_V = 7,64 md is estimated using *Equation 5*.

Table 1. Pressure data for field example 1

t, h	P_{wf}, psia	ΔP, psia	$t^*\Delta P'$, psia	t, h	P_{wf}, psia	ΔP, psia	$t^*\Delta P'$, psia
0,0	2266,0	0,0		4,0	2178,0	88,0	60,0
0,5	2255,0	11,0	11,5	4,5	2170,0	96,0	56,3
1,0	2243,0	23,0	24,5	5,5	2161,0	105,0	46,8
1,6	2228,0	38,0	40,0	6,0	2157,0	109,0	48,0
2,0	2218,0	48,0	45,0	6,5	2153,0	113,0	52,0
2,5	2208,0	58,0	52,5	7,0	2149,0	117,0	49,0
3,0	2197,0	69,0	69,0	7,5	2146,0	120,0	52,5
3,5	2185,0	81,0	66,5	8,0	2142,0	124,0	48,0
				8,5	2140,0	126,0	

Step 6. An I_A value of 0,92 is estimated with *Equation 47*. This value is not significantly less than 1, but it still indicates an anisotropic reservoir.

Step 7. Since the value of the mecanical skin is unknown because the initial radial flow is not seen, the partial penetration skin can be calculated using using the following expression (Brons and Marting, 1961):

$$s_c = \left(\frac{1}{h_p/h} - 1 \right) [\ln h_D - G] \qquad (49)$$

for spherical flow,

$$h_D = \left(\frac{k_H}{k_V} \right)^{0.5} \left(\frac{h}{2r_w} \right) \qquad (50)$$

For hemispherical flow, the 2 in the denominator of *Equation 50* ought to be removed.

$$G = 2.948 - 7.363 \left(\frac{h_p}{h} \right) + 11.45 \left(\frac{h_p}{h} \right)^2 - 4.675 \left(\frac{h_p}{h} \right)^3 \qquad (51)$$

then, $h_D = 659,25$; $G = 1,57$ and $s_c = 7,46$ are estimated.

Simulated example 1

Using a numerical simulator a pressure buildup test for an oil well with partial penetration has been simulated using the same reservoir parameters presented by Joseph and Koederitz (1985), (Table 2) and the pressure data is provided in Table 3.

Solution

Step 1. The pressure and pressure derivative plot is shown in Figure 9. On the *initial radial flow regime* values of $(t*\Delta P')_{r1}= 20$ psi, $(\Delta P)_{r1}= 348,3$ psi and $t_{r1} = 0,009$ h are read. A radial permeability value of 81,1 md is calculated using *Equation 15* and a skin factor of 5,15 is found by means of *Equation 16*.
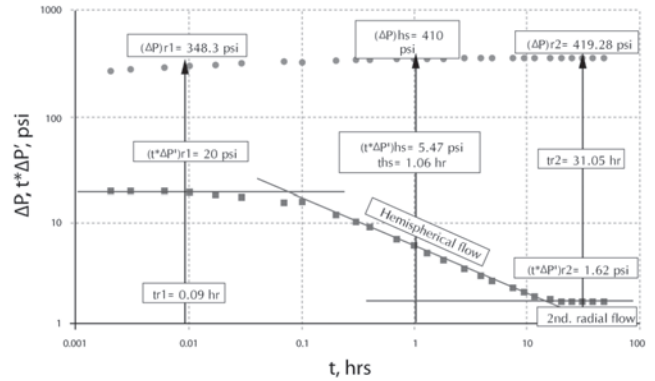

Figure 9. Pressure and pressure derivative plot for simulated example 1

Step 2. From the -½-slope straight line, at $t_{hs} = 1,06$ h, the following data are obtained: $(t*\Delta P')_{hs}= 1,62$ psi and $(\Delta P)_{hs}= 419,28$ psi. k_{hs} of 54,7 md can be calculated using *Equation 33*.

Step 3. A value of s_{hs} of 0,41 is estimated with *Equation 39*.

Table 2. Reservoir, well and rock data used for simulation examples

Simulated example 1 (Oil well)				Simulated example 2 (Gas well)			
Property	Value	Property	Value	Property	Value	Property	Value
k_H, md	80	r_w, ft	0,417	h, ft	100	r_w, ft	0,3
k_V, md	24	p_{wf}, Psia	3850	h_p, ft	13	q_g, Mscf	2000
kv/kH	0.3	q, bpd	248	ø, %	25	μ_g, cp	0,0267
h, ft	350	μ, cp	2,18	c_f, psi-1	3,0 *10-6	z_i	1,003
h_p, ft	28	B_o, rb/STB	1,19	$m(P_i)$, psi2/cp	935369677.7	T, °R	671,67
ø, %	8	s	5	kh, md-ft	3000		
c_o, psi-1	1,03x10-5	C_D	0				
c_f, psi-1	1,7x10-6	t_p, h	200				
c_t, psi-1	1,2x10-5						

Table 3. Pressure data for simulated example 1

t, h	P_{wf}, psia	ΔP, psia	$t*\Delta P'$, psia	t, h	P_{wf}, psia	ΔP, psia	$t*\Delta P'$, psia
0	4145,7	304,2	20,2	1,3	4252,6	411,1	4,9
0,002	4154,5	313,1	20,2	1,8	4254,1	412,6	4,2
0,003	4165,6	324,2	20,2	2,8	4255,7	414,3	3,4
0,006	4178,9	337,4	20,1	3,9	4256,8	415,3	2,9
0,01	4189,8	348,3	19,6	4,9	4257,4	415,9	2,6
0,017	4200,2	358,8	18,6	7,5	4258,4	416,9	2,2
0,029	4210	368,6	17,3	9,4	4258,8	417,4	2
0,07	4224,2	382,7	15,5	11,7	4259,2	417,8	1,8
0,1	4219,1	377,7	15,8	16,2	4259,8	418,3	1,7
0,2	4235,8	394,4	11,7	20,1	4260,1	418,7	1,6
0,3	4240,6	399,2	10	25	4260,4	419	1,6
0,4	4243,7	402,3	8,8	31,1	4260,7	419,3	1,6
0,7	4248,8	407,3	6,7	38,6	4261	419,6	1,6
1	4250,8	409,4	5,8	48	4261,3	419,9	1,6

Step 4. At t_{r2}=31,05 hr (late radial flow regime), we read $(t*\Delta P')_{r2}$= 1,62 psi and $(\Delta P)_{r2}$= 419,28 psi. Then, k_r of 80,1 md is determined with *Equation 44* and s_t of 121,8 can be calculated using *Equation 45*.

Step 5. k_V is found to be 25,79 md using *Equation 34*.

Step 6. An I_A of 0,32 is determined with *Equation 47*.

Step 7. Since $b = 0,08$, a partial penetration skin of 57,42 is found with *Equation 48*.

Table 4. Pseudopressure data for simulated example 2

Δt, (h)	m(P), (psi2/cp)	$\Delta m(P)$, (psi2/cp)	$t*\Delta m(P)'$ (psi2/cp)	Δt, (h)	m(P), (psi2/cp)	$\Delta m(P)$, (psi2/cp)	$t*\Delta m(P)'$, (psi2/cp)
0,0001	927562604,5	7807073,188	1986070	0,1600	916444706,1	18924971,56	464872
0,0002	926180835,8	9188841,822	2034200	0,2261	916296574,7	19073102,98	399896
0,0004	924770335,2	10599342,49	2052510	0,3193	916170672,4	19199005,28	355218
0,0006	923948349,4	11421328,29	2037370	0,4511	916052184	19317493,66	330527
0,0008	923368344,2	12001333,52	2015680	0,6372	915941108,1	19428569,56	320546
0,0014	922231170,5	13138507,14	1945070	1	915800421,6	19569256,03	318028
0,0025	921150390,7	14219286,96	1839910	1,4	915693062,9	19676614,75	318283
0,0101	918894311,6	16475366,05	1421470	2	915582008,8	19787668,87	318560
0,0201	918015635,3	17354042,34	1141880	2,6	915500573,4	19869104,28	318626
0,0402	917330040,9	18039636,79	870852	3,6	915396933,6	19972744,11	318624
0,0568	917055874,8	18313802,86	750153	4,6	915319207,5	20050470,13	318604
0,0802	916818791,3	18550886,42	641988	7	915189671,5	20180006,17	318577
0,1133	916615072,1	18754605,61	546606	9,7	915086049,3	20283628,39	318567

Table 5. Comparison of results between conventional and TDS methods

Parameters	Field example 1		Simulated example 1 - oil		Simulated example 2 – gas	
	Conventional	TDS	Conventional	TDS	Conventional	TDS
C, bbl/psi	16,01	16,01	-	-		
ksp, md	7,81	8,05	-	-		
ssp	0	0	-	-		
khs, md	-	-	52,51	54,7	9,27	8,64
shs	-	-	0	0	-0,84	-0,84
kr1, md	-	-	81,22	81,1	35,8	35,6
kr2, md	8,19	9,04	80,78	80,1	30,82	29,9
sr1	-	-	4,86	5,15	-4,6	-4,95
sr2	-5,03	-5,26	119	121,8	23,5	22,65
kV, md	7,10	6,38	22,18	25,79	0,84	0,72
sc (or sc')	7,46	56,93	57,57	36,38	36,73	

Simulated example 2

Table 4 presents synthetic pseudopressure data for drawdown test in a gas well generated with the data given in Table 2. Estimate permeabilities, pseudoskin and skin factors using *TDS* technique.

Solution

Step 1. Figure 10 presents the pressure and pressure derivative plot for this simulated example. Values of $(t^*\Delta m(P'))_{r1}$= 2052510 psi^2/cp, $(\Delta m(P))_{r1}$= 10599342,5 psi^2/cp and t_{r1} = 0,0004 h are read. A radial permeability value of 35,8 md is calculated using *Equation A.10* and a skin factor of -4,95 is determinated with *Equation A.11*.
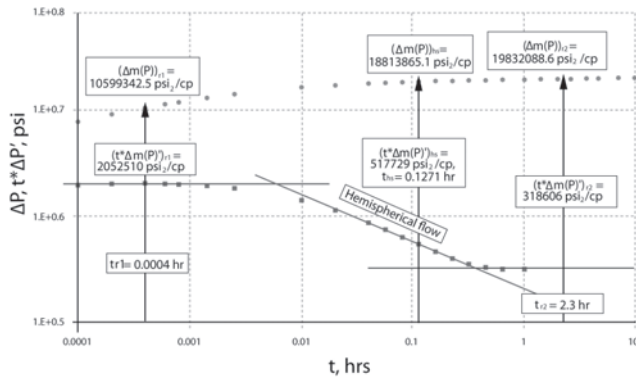

Figure 10. Pseudopressure and pseudopressure derivative plot for simulated example 2

Step 2. From the -½-slope straight line, at t_{hs}=0,127128 hr, the following data are obtained: $(t^*\Delta m(P'))_{hs}$= 517729 psi^2/cp and $(\Delta m(P))_{hs}$=18813865,1 psi^2/cp. k_{hs} of 8,64 md can be calculated using *Equation A.13*.

Step 3. A value of s_{hs} of -0,84 is estimated with *Equation A.15*.

Step 4. At t_{r2}= 2,3 h (late radial flow regime), we read $(t^*\Delta P')_{r2}$= 318606 psi^2/cp and $(\Delta P)_{r2}$= 19832088,6 psi^2/cp. Then, k_r of 29,99 md is found using *Equation A.16* and s_t' of 22,5 is determined by means of Equation *A.17*

Step 5. k_V is found to be 0,72 md using *Equation 34*.

Step 6. I_A = 0,024 is determined with *Equation 47*.

Step 7. Since b = 0,13, a partial penetration skin of 36,73 is calculated using *Equation 48*.

Note: Although not shown here, the examples were also worked using conventional techniques and reported in Table 5 for comparison purposes. Permeabilities may be verified using either *Equations 17.a, 20, 21, 40.a, 42,* or *43* for the given case. Also, for gas wells, it should be taken into account that pseudoskin factors and rapid flow conditions have to be included to find the true skin factor as explained with great detail in Núñez-García *et al.* (2003).

CONCLUSIONS

- Analytical equations based upon pressure derivative for a homogeneous reservoir are presented for well test interpretation of vertical gas and oil wells partially completed and partially penetrated including wellbore storage and skin effects.

- The log-log plot of pressure derivative versus time provides much more information about partially completed or partially penetrated vertical wells than conventional methods based on pressure vs. time plots.

- A straight line with slope of negative one-half was identified as the unique characteristic of the pressure derivative plot if spherical/hemispherical flow regime is present.

- The straight line corresponding to the spherical or hemispherical flow regime can be used to calculate the spherical/hemispherical permeability and spherical/hemis-pherical skin. These parameters are necessary to estimate vertical permeability.

- Using radial coordinates (*Equation 11.b*), either the spherical or hemispherical flow regime is completely masked for dimensionless wellbore storage values greater than 10 and penetration ratios higher than 40 .

- The Tiab's Direct Synthesis Technique was extended for vertical gas and oil wells with partial completion or partial penetration and its practical step-by-step procedure is presented. It leads to more accurate results compared with conventional methods.

REFERENCES

Abbott, W. A., Collins, T., Tippie, D. B., Van Pollen, H. K., 1978. "Practical Application of Spherical Flow Transient Analysis" *53rd Annual Fall Technical Conference and Exhibition of the SPE of AIME*. TX, U.S.A. SPE 7435.

Al-Hussainy, R., Ramey, H. J. and Crawford P. B., 1966. "The Flow of Real Gases Through Porous Media", *JPT,* 624-36; Trans., AIME, 237.

Boussalem, R., Tiab, D., and Escobar, F. H., 2002. "Effect of Mobility Ratio on the Pressure and Pressure Derivative Behaviors of Wells in Closed Composite Reservoirs". *SPE Western Regional Mtg./AAPG Pacific Section Joint Mtg.*, Anchorage, Alaska. SPE 76781.

Bringham, W. E., Peden, J. M., Ng. K. F., and O'Neill, N., 1980. "The Analysis of Spherical Flow with Wellbore Storage". *55th Annual Technical Conference and Exhibition,* Dallas, Texas, U.S.A.. SPE 9294.

Brons, F. and Marting, V. E., 1961. "The Effect of Restricted Fluid Entry on Well Productivity," Trans., AIME, 222.

Chacón, A., Djebrouni, A. and Tiab, D., 2004. "Determining the Average Reservoir Pressure from Vertical and Horizontal Well Test Analysis Using the Tiab's Direct Synthesis Technique". *SPE Asia Pacific Oil and Gas Conference and Exhibition*, Perth, Australia. SPE 88619.

Chatas, A. T., 1966. "Unsteady Spherical Flow in Petroleum Reservoirs", SPEJ, 102.

Cherifi, M., Tiab, D., and Escobar, F. H., 2002. "Determination of Fracture Orientation by Multi-Well Interference Testing". *SPE Asia Pacific Oil and Gas Conference and Exhibition*, Melbourne, Australia. SPE 77949.

Culham, W. E., 1974. "Pressure Buildup Equations for Spherical Flow Regime Problems", SPEJ 545.

Earlougher, R.C., Jr., 1997. "Advances in Well Test Analysis", *Monograph Series*, 5, SPE, Dallas, TX., U.S.A..

Engler, T. and Tiab, D., 1996. "Analysis of Pressure and Pressure Derivative without Type Curve Matching, 4. Naturally Fractured Reservoirs". *J. of Petroleum Scien. and Engineering* ,15, 127-138.

Escobar, F. H., Tiab, D. and Berumen-Campos, S., 2003. "Well Pressure Behavior of a Finite-Conductivity Fractured Well Intersecting a Sealing Fault". *Oil and gas SPE Asia Pacific Conference and Exhibition*, Jakarta, Indonesia. SPE 80547.

Escobar, F. H., Muñoz, O.F. and Sepúlveda J.A., 2004. "Horizontal Permeability Determination from the Elliptical Flow Regime for Horizontal Wells". *CT&F – Ciencia, Tecnología y Futuro*, 2 (5): 83-95.

Escobar, F. H., Saavedra, N. F., Escorcia, G. D., and Polanía, J. H., 2004. "Pressure and Pressure Derivative Analysis Without Type-Curve Matching for Triple Porosity

Reservoirs". *SPE Asia Pacific Oil and Gas Conference and Exhibition (APOGCE)*, Perth, Australia. SPE 88556.

Escobar, F. H., Saavedra, N.F., Hernández, C.M., Hernández, Y.A., Pilataxi, J.F., and Pinto, D.A., 2004. "Pressure and Pressure Derivative Analysis for Linear Homogeneous Reservoirs without Using Type-Curve Matching". *28th Annual SPE International Technical Conference and Exhibition*, Abuja, Nigeria, Aug. 2-4. SPE 88874.

Escobar, F. H., Tiab, D. and Jokhio, S.A., 2003. "Characterization of Leaky Boundaries from Transient Pressure Analysis". *Production and Operations Symposium*, Oklahoma City, Oklahoma, U.S.A., March 23-25. SPE 80908.

Guira, B. Tiab, D., and Escobar, F. H., 2002. "Pressure Behavior of a Well in an Anisotropic Reservoir Near a No-Flow Boundary". *Proceedings, SPE Western Regional Mtg./AAPG Pacific Section Joint Meeting*, Anchorage, Alaska. SPE 76772.

Hachlaf, H, Tiab, D. and Escobar, F. H., 2002. "Effect of Variable Injection Rate on Falloff and Injectivity Tests". *SPE Western regional Meeting/AAPG Pacific Section Joint Meeting*, Anchorage, Alaska. SPE 76714.

Ispas, V., and Tiab, D., 1999. "New Method of Analyzing the Pressure behavior of a Well Near Multiple Boundary System". *Latin American and Caribbean Petroleum Engineering Conference*, Caracas, Venezuela, April 21-23, SPE 53933.

Jokhio, S. A., Tiab, D., Hadjaz, A. and Escobar, F. H., 2001. "Pressure Injection and Falloff Analysis in Water Injection Wells Using the Tiab's Direct Synthesis Technique". *SPE Permian Basin oil and Gas recovery conference*, Midland, TX., USA. SPE 70035.

Joseph, J. A.,1983. "Unsteady-State Cylindrical and Spherical flow in Porous Media," *Report No. USDI G1124129, Missouri Mining and Mineral Resources Research Inst., Rolla*, MO.

Joseph, J.A., 1984. "Unsteady-State Cylindrical, Spherical and Linear flow in Porous Media" *Ph.D. Dissertation*, University of Missouri-Rolla.

Joseph, J. A., and Koederitz, L. F., 1985. "Unsteady-State Spherical Flow With Storage and Skin," SPEJ, 804-822.

Khelifa, M., Tiab, D., and Escobar F. H., 2002. "Multirate Test in Horizontal Wells". *SPE Asia Pacific Oil and Gas Conference and Exhibition*. Melbourne, Australia. SPE 77951.

Miller, F. G., 1962. "Theory of Unsteady-State influx of Water in Linear Reservoirs," *J. Inst. Pet.* .48, (467): 365-379.

Moncada, K., 2004. "Application of TDS Technique to Calculate Vertical and Horizontal Permeabilities for Vertical Wells with Partial Completion and Partial Penetration". M.S. Thesis. The University of Oklahoma.

Mongi, A., and Tiab, D., 2002. "Application of Tiab's Direct Synthesis Technique to Multi-Rate Tests" *Presented at the 2000 SPE/AAPG Western Regional Mtg. held in Long Beach*, California, 19–23. SPE 62607.

Morán, J. H and Finlklea, E.E., 1962. "Theoretical Analysis of Pressure Phenomena Associated with the Wireline Formation Tester", Trans AIME 225, 899.

Muskat, M., 1932. "Partially Penetrating Wells in Isotropic Formations; Potential Distribution," Physics, 329.

Núñez-García, Walter, Tiab, D., and Escobar, F. H., 2003. "Transient Pressure Analysis for a Vertical Gas Well Intersected by a Finite-Conductivity Fracture". *SPE Production and Operations Symposium*, Oklahoma City, OK., U.S.A., 23–25. SPE 80915.

Odeh, A. S., 1968. "Steady-State Flow Capacity of Wells with Limited Entry to Flow," Trans., AIME, 243.

Proett, M. A. and Chin, W. C., 1998. "New Exact Spherical Flow Solution with Storage for Early-time Test Interpretation with Applications to Early-Evaluation Drillstem and Wireline Formation Testing," *SPE Permian Basin Oil and Gas Recovery Conference*, Midland, TX., USA. SPE 39768.

Raghavan R. and Clark K. K., 1975. "Vertical Permeability from Limited Entry Flow Tests in Thick Formations," *SPEJ*, 65-73.

Streltsova-Adams T. D., 1979. "Pressure Drawdown in a Well with Limited Entry," *Soc. Petroleum Engineer., J.*, 1469-1476.

Tiab, D., 1993. "Analysis of Pressure and Pressure Derivative without Type-Curve Matching: 1- Skin Factor and Wellbore Storage". *Production Operations Symposium*, Oklahoma City, OK., March 21-23. SPE 25423, 203-216. Also, *J. Petroleum Scien. and Engineer.,* 171-181.

Tiab, D., 1994. "Analysis of Pressure Derivative without Type-Curve Matching: Vertically Fractured Wells in Closed Systems". *J. Petroleum Scien. and Engineer.,* 323-333. *1993 SPE Western Regional Mtg.*, Anchorage, Alaska.

Tiab, D., Azzougen, A., Escobar, F. H., and Berumen, S., 1999. "Analysis of Pressure Derivative Data of a Finite-Conductivity Fractures by the *'Direct Synthesis Technique'*." *Mid-Continent Operations Symposium* Oklahoma City, OK., March 28-31. SPE 52201: *Latin American and Caribbean Petroleum Engineer., Conference*, Caracas, Venezuela, April 21-23.

Tiab, D., y Escobar, F. H., 2003. "Determinación del Parámetro de Flujo Interporoso de un Gráfico Semilogarítmico". *X Congreso Colombiano del Petróleo*. Bogotá, Colombia, 2005.

Zamora, R. A. and Nese, S. L., 2005. "Análisis de Presión y Derivada de Presión en Yacimientos de Gas con Completamiento y Penetración Parcial". *B.S. Thesis.* Universidad Surcolombiana. Neiva, Huila, Colombia.

APPENDIX A

Gas Equations

Al-Hussainy (1966) introduced the pseudopressure defined as:

$$m(P) = 2 \int_{P_m}^{P} \frac{P}{\mu(P)z(P)} dP \tag{A.1}$$

The pseudopressure difussivity equation is:

$$\frac{1}{r^2} \frac{\partial}{\partial r}\left(r^2 \frac{\partial m(P)}{\partial r}\right) = \frac{\phi \mu c_g}{k_{sp}} \frac{\partial m(P)}{\partial t} \tag{A.2}$$

The dimensionless pseudopressure in radial, spherical and hemispherical symmetries, respectively, are:

$$m(P)_{Dr} = \frac{k_r h}{1422.52qT} \Delta m(P) \tag{A.3}$$

$$m(P)_{Dsp} = \frac{k_{sp} r_{sw}}{711.26qT} \Delta m(P) \tag{A.4}$$

$$m(P)_{Dhs} = \frac{k_{hs} r_{sw}}{1422.52qT} \Delta m(P) \tag{A.5}$$

The dimensionless pseudopressure derivatives in radial, spherical and hemispherical symmetries, respectively, are:

$$\left(t_D * m(P)_D{}'\right)_r = \frac{k_r h}{1422.52qT}\left(t * \Delta m(P)'\right) \tag{A.6}$$

$$\left(t_D * m(P)_D{}'\right)_{sp} = \frac{k_{sp} r_{sw}}{711.26qT}\left(t * \Delta m(P)'\right) \tag{A.7}$$

$$\left(t_D * m(P)_D{}'\right)_{hs} = \frac{k_{hs} r_{sw}}{1422.52qT}\left(t * \Delta m(P)'\right) \tag{A.8}$$

$$C = 0.419 \frac{q_g T}{\mu_{gi}}\left(\frac{t}{\Delta m(P)}\right)_N \tag{A.9}$$

$$k_{r1} = k_H = 711.26 \frac{q_g T}{h_p (t * \Delta m(P)')_{r1}} \tag{A.10}$$

$$s_{r1} = s'_m = 0.5\left[\frac{(\Delta m(P))_{r1}}{(t * \Delta m(P)')_{r1}} - \ln\left(\frac{k_r t_{r1}}{\phi \mu c_t r_w^2}\right) + 7.43\right] \tag{A.11}$$

$$k_{sp} = \left(12355.73 \frac{q_g T}{(t * \Delta m(P)')_{sp}} \sqrt{\frac{\phi \mu c_t}{t_{sp}}}\right)^{2/3} \tag{A.12}$$

$$k_{hs} = \left(24711.46 \frac{q_g T}{(t * \Delta m(P)')_{hs}} \sqrt{\frac{\phi \mu c_t}{t_{hs}}}\right)^{2/3} \tag{A.13}$$

$$s_{sp} = 34.74 \sqrt{\frac{\phi \mu c_t r_{sw}^2}{k_{sp} t_{sp}}} \left[\frac{(\Delta m(P))_{sp}}{2(t * \Delta m(P)')_{sp}} + 1\right] - 1 \tag{A.14}$$

$$s_{hs} = 34.74 \sqrt{\frac{\phi \mu c_t r_{sw}^2}{k_{sp} t_{sp}}} \left[\frac{(\Delta m(P))_{hs}}{2(t * \Delta m(P)')_{hs}} + 1\right] - 1 \tag{A.15}$$

$$k_{r2} = k_H = 711.26 \frac{q_g T}{h(t * \Delta m(P)')_{r2}} \tag{A.16}$$

$$s'_{r2} = s_t = 0.5\left[\frac{(\Delta m(P))_{r2}}{(t * \Delta m(P)')_{r2}} - \ln\left(\frac{k_r t_{r2}}{\phi \mu c_t r_w^2}\right) + 7.43\right] \tag{A.17}$$